ELSEVIER

Journal of Nuclear Materials 248 (1997) 191–195

journal of nuclear materials

Radiation damage of UO_2 by high-energy heavy ions

Kimio Hayashi *, Hironobu Kikuchi, Kousaku Fukuda

Fuel Irradiation & Analysis Lab., Japan Atomic Energy Research Institute, Tokai-mura, Ibaraki-ken 319-11, Japan

Abstract

In connection with the rim effect of high-burnup light water reactor (LWR) fuel, a series of experimental studies on the radiation damage of UO_2 was conducted by irradiation of high energy heavy ions in the order of 100 MeV. Sliced UO_2 pellets for LWR were irradiated at ambient temperatures below 200°C, with 100–300 MeV iodine and 100 MeV nickel ions over a fluence range of 2×10^{-17}–1.8×10^{20} ions/m^2. The lattice parameter changes ($\Delta a/a_0$) at the surface, induced by 100 MeV iodine and nickel irradiations were reasonably scaled by the displacement per atom (dpa), which accounted the nuclear energy deposition only. The changes, $\Delta a/a_0$, however, could not be scaled by the electronic energy deposition at the surface. In the 100–300 MeV iodine irradiation, the lattice parameter slightly increased with increasing incident ion energy. The above results suggest in total that the defect formation corresponding to the lattice parameter change was mainly due to the nuclear energy deposition under the present experimental conditions, with an additional contribution of the electronic energy deposition. © 1997 Elsevier Science B.V.

1. Introduction

One of the most important problems on high burnup fuels for light water reactors (LWRs) is the so-called rim effect, or a microstructural change forming a grain subdivision. Recent studies on the rim effect [1–5] revealed that this phenomenon is related to radiation damage introduced by energetic fission fragments at lower temperatures in the pellet rim region.

The present authors have made a series of high-energy ion irradiation experiments in an energy region comparable to that of the fission products [6–9]. In this energy region, most of the projectile energy is transferred to the target atoms as electronic energy deposition through inelastic collisions, rather than nuclear energy deposition through elastic collisions, between the incident ions and the target atoms, as described in Section 2.

Preliminary results were already published as a paper [6] and annual progress reports [7–9]. The present paper deals with the radiation damage of UO_2 by irradiation of 100–300 MeV iodine and 100 MeV nickel ions, using revised data from repeated irradiations and X-ray diffraction analyses, which are described in Appendix A. The obtained results are discussed from a viewpoint of contributions of the nuclear and electronic energy depositions to the generation of the lattice defects.

2. Theoretical derivation of nuclear and electronic energy depositions and dpa

The electronic and nuclear stopping powers are shown in Fig. 1 as a function of the incident energy of the iodine ions implanted into UO_2. The calculation was made by a code, EDEPJR-87 [10], which is an extension of the EDEP-1 code [11,12] to the high energy region for universal application. Fig. 1 clearly indicates that the electronic stopping power is much larger than the nuclear energy deposition in the energy range of the fission fragments, i.e., about 60–100 MeV.

Next, the nuclear and electronic energy depositions, $D_n(x)$ and $D_e(x)$ (MeV/μm), respectively, were calculated as a function of the depth, x (μm), using the EDEPJR-87 code. The results are summarized in Table 1, and depicted in Fig. 2 for 100 MeV iodine irradiation. The peak position of the nuclear energy deposition lies at 6.3 μm from the surface. It was assumed here that the constituent atoms were homogeneously distributed in the UO_2 with a 95% theoretical density (TD), which was used in the present experiment.

* Corresponding author. Tel.: +81-29 282 6083; fax: +81-29 282 6442.

PII S0022-3115(97)00119-0

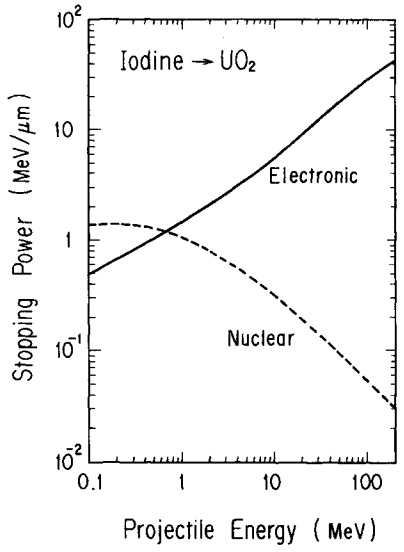

Fig. 1. Nuclear and electronic stopping powers as a function of the projectile energy, calculated by the EDEPJR-87 code [10] for ^{127}I ion implantation into UO_2 of 95% TD.

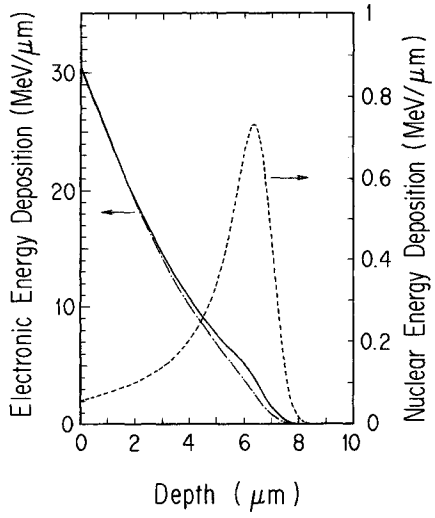

Fig. 2. Depth distributions of nuclear and electronic energy depositions, calculated by the EDEPJR-87 code for 100 MeV ^{127}I ion implantation into UO_2 of 95% TD. The dash-dotted line of the electronic energy deposition represents the contribution of the incident iodine ions only, while the solid line represents the sum of both contributions of the incident ions and the recoiled atoms.

Furthermore, based on the NRT model [13], the atomic concentration of displaced uranium and oxygen atoms, $Cd_U(x)$ and $Cd_{Ox}(x)$, were obtained from the calculated nuclear energy deposition in a dimensionless unit of displacements per atom for uranium and oxygen, i.e., dpa-U and dpa-Ox, respectively, as follows:

$$Cd_U(x) = \frac{\phi t}{n_U} \frac{\kappa f_U D_n(x)}{2E_d(U)}, \quad (1)$$

$$Cd_{Ox}(x) = \frac{\phi t}{n_{Ox}} \frac{\kappa f_{Ox} D_n(x)}{2E_d(Ox)}, \quad (2)$$

where a constant ion flux, ϕ (m^{-2} s^{-1}), is assumed over the irradiation time, t (s), for simplicity in the expression of Eqs. (1) and (2). Atomic densities of 2.44×10^{28} and 4.88×10^{28} m^{-3} for uranium (n_U) and oxygen (n_{Ox}), respectively, were used for the present UO_2 specimen with 95% TD; and 40 and 20 eV were adopted for the displacement (threshold) energies of uranium ($E_d(U)$) and oxygen ($E_d(Ox)$), respectively, based on a calculation by Soullard et al. [14,15]. The displacement efficiency, κ, is assumed to be 0.8, following the NRT model [13]. The partition fractions of the nuclear energy deposited to uranium and oxygen atoms, f_U and f_{Ox}, were assumed to be 0.423 and 0.577, respectively, for iodine ion irradiation, based on the calculation by Soullard et al. [14,15]. Similarly, for nickel

Table 1
Typical results of calculation by the EDEPJR-87 code [10], and irradiation conditions

	Iodine ion			Nickel ion
	100 MeV	200 MeV	300 MeV	100 MeV
Mean projected range (μm)	6.8	9.5	11.4	6.9
Peak depth of nuclear energy deposition (μm)	6.3	9.0	11.0	6.6
Stopping power (MeV/μm)	30	44	58	29
Electronic energy deposition at surface [a] (10^{31} eV/m^3)	30	44	58	29
DPA at surface [a]				
Uranium atom	0.10	0.059	0.043	0.020
Oxygen atom	0.14	0.081	0.058	0.027
Ion flux (10^{15} ions/m^2 s)	0.83–4.6	1.1–1.8	0.037–0.052	4.6–6.7
Ion fluence (10^{19} ions/m^2)	0.035–18	0.020–4.0	0.020–0.040	0.11–16
Beam heating power (W) [b]	0.26–1.4	0.69–1.1	0.035–0.049	1.4–2.1
Irradiation temperature (°C)	< 200	< 200	< 200	< 200

[a] At an ion fluence of 1×10^{19} ions/m^2.
[b] For the ion beam spot of 5 mm in diameter.

ion irradiation, the corresponding partition fractions were assumed to be 0.4265 and 0.5735, as in the case for the median light fission products [14,15]. Details of the derivation process will be described elsewhere.

3. Experimental procedure

3.1. Specimens

Specimens used were sintered (polycrystalline) UO_2 discs, 10.4 mm in diameter and about 1 mm in thickness, which had been sliced from pellets of commercial LWR fuel. The density of the specimens was 95% [16] of the theoretical density of UO_2 (10.96 Mg/m^3), and the average grain size was about 14 μm [16]. The specimen discs were polished with emery paper and diamond paste of about 1 μm particle size. Subsequently, the specimens were annealed in flowing Ar–4% He gas at 1400 or 1500°C for 2 h, so as to remove the surface damage due to polishing [17], although no change due to polishing was detected in the lattice parameter obtained by X-ray diffractometry [7]. The lattice parameter of the un-irradiated specimens, a_0, was 547.05 ± 0.05 pm, which corresponds to $UO_{2.00}$ [18].

3.2. Irradiation

Irradiations were made at ambient temperatures using the Tandem Accelerator of the Tokai Establishment of the Japan Atomic Energy Research Institute (JAERI) with 100 MeV $^{127}I^{7+}$, 200 MeV $^{127}I^{12+}$, 300 MeV $^{127}I^{22+}$, and 100 MeV $^{58}Ni^{6+}$ ions. In order to suppress the effect of ion beam heating at the beam incidence side surface, the rear side of the specimen was cooled by water that was kept at about 20°C. The temperature at the beam-incidence side surface was monitored during irradiation by a low-temperature infrared pyrometer with a PbS sensor, and the temperature was measured to be lower than 200°C, which is the detection limit of the pyrometer. The ion fluence was measured by a current integrator, and the ion flux was evaluated as the time average thereof. The pressure in the target chamber was kept below 3×10^{-3} Pa. Main irradiation conditions are summarized in Table 1.

3.3. Analysis of irradiated specimens

Lattice parameters of the irradiated specimens were measured by a conventional X-ray diffraction apparatus, RU-200B of Rigaku, with a Cu Kα beam. In order to limit the X-ray analysis area within the ion beam spot (5 mm in diameter), the specimens were masked with a molybdenum plate, which was 0.2 mm in thickness and had a central hole of 2 or 3 mm in diameter. The lattice parameter was obtained by a least-squares fitting method for seven diffraction lines at higher angles (78, 94, 105, 113, 126, 135 and 138° in 2θ).

The penetration depth of the X-ray (Cu Kα) into the UO_2 specimen was estimated to be about 2 μm, where the linear absorption coefficient for UO_2 was calculated by Bragg's law, using mass absorption coefficients of 30.6 and 1.10 m^2/kg [19] for uranium and oxygen, respectively.

4. Results and discussion

4.1. MeV nickel and iodine irradiation

Lattice parameter changes, $\Delta a/a_0$, observed after the irradiation are plotted in Fig. 3 as a function of displacement per uranium atom (dpa-U) at the surface, and as a function of the electronic energy deposition at the surface in Fig. 4. Here, the results calculated in Section 2 were used. A more elementary relationship between the lattice parameter change and the ion fluence is given below in Fig. 5 for the 100 MeV iodine irradiation, and was already given in Ref. [7] for the nickel irradiation.

In Fig. 3, the plots for the nickel and iodine irradiation agree well with each other. This result indicates that the lattice parameter change, which is considered to have reflected the point defect concentration [20] at the surface, can be scaled by the dpa values, namely by the normalized nuclear energy depositions. Essentially the same agreement will be obtained by scaling with the dpa of oxygen, dpa-Ox, or with the nuclear energy deposition at the surface.

In contrast, the plots for the nickel and iodine irradiation are far separated in Fig. 4, implying that the damage effect cannot be scaled by the electronic energy deposition at the surface.

These results of scaling indicate that the damage effect relating to the lattice parameter change of UO_2 was mainly induced by the nuclear energy deposition.

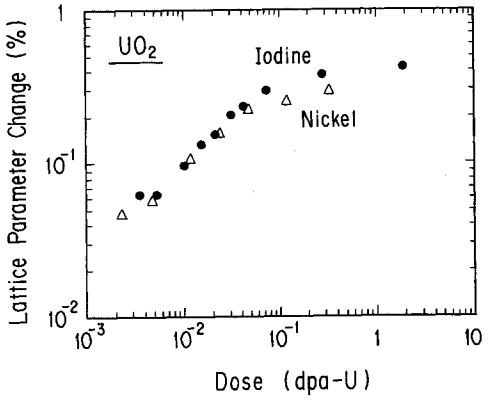

Fig. 3. Lattice parameter changes of UO_2 irradiated with 100 MeV ^{58}Ni and ^{127}I ions as a function of displacement per uranium atom at the surface.

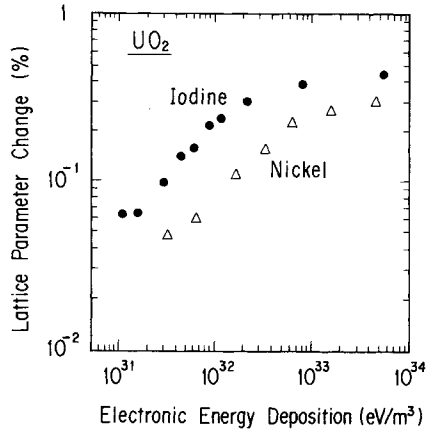

Fig. 4. Lattice parameter changes of UO_2 irradiated with 100 MeV ^{58}Ni and ^{127}I ions as a function of the electronic energy deposition at the surface.

4.2. 100–300 MeV iodine irradiation

Lattice parameter changes are plotted as a function of the ion fluence in Fig. 5. This figure shows that the lattice parameter change increased with increasing incident ion energy in the range of 100–300 MeV.

As already seen in Fig. 1, the electronic stopping power increases, while the nuclear decreases, with increasing incident energy in the energy region around 100 MeV. Considering the above-estimated X-ray penetration depth of 2 μm and the depth profiles of the nuclear and electronic energy depositions (Fig. 2), the nuclear and electronic energy depositions at the surface region relevant to the surface X-ray diffraction can be roughly approximated by the nuclear and electronic stopping powers, respectively.

Thus, the observed increase in the lattice parameter change with the incident energy is opposite to the deceasing tendency of the nuclear energy deposition. This suggest that the defect formation cannot be ascribed to the nuclear energy deposition only. In contrast, the increase in the lattice parameter change is consistent with the increasing tendency of the electronic energy deposition. This result suggests that the electronic energy deposition made an additional contribution to the lattice parameter change in the surface region.

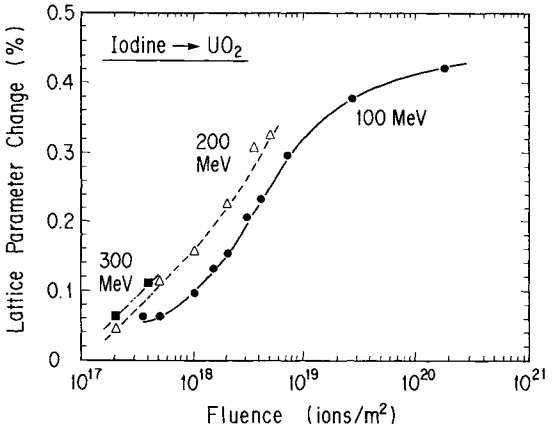

Fig. 5. Lattice parameter changes of UO_2 irradiated with 100, 200 and 300 MeV ^{127}I ions as a function of ion fluence.

It is noted in Table 1 that the ion beam heating power was different for the different energies. Annealing of irradiation-induced defects was not observed for UO_2 at temperatures between room temperature and 150°C [20,21], but was observed between 150 and 250°C [20]. It is suspected, therefore, that the diffusion of the radiation-induced lattice defects resulted in broadening of the instantaneous depth profile of the induced defect concentration, and consequently in modifying the lattice parameter change at the surface, even at the present irradiation temperatures below 200°C. However, the beam heating power for the 200 MeV irradiation (0.69–1.1 W) is close to that for the 100 MeV irradiation (0.26–1.4 W). Thus, the observed larger lattice parameter changes for 200 MeV over 100 MeV irradiation over the whole ion fluence range cannot be ascribed to the beam heating effect, namely the effect of the irradiation temperature.

In summary, the present finding of the additional lattice parameter change suggests the formation of lattice defects due to the electronic energy deposition. The suggestion was already observed in a discrepancy between the depth profiles of the lattice parameter change and the nuclear energy depositions, in the vicinity of the surface [9].

5. Conclusions

In order to study the radiation damage processes in UO_2 by fission fragments, irradiation was made on UO_2 with 100–300 MeV iodine and 100 MeV nickel ions. Sliced UO_2 pellets for LWR were irradiated at ambient temperatures below 200°C over a dose range of 2×10^{-17}–1.8×10^{20} ions/m^2. After irradiation, the specimens were analyzed by X-ray diffractometry.

(1) The lattice parameter changes, $\Delta a/a_0$, induced by 100 MeV nickel and iodine irradiation were reasonably scaled by the dpa at the surface, which accounted for the nuclear energy deposition only.

(2) The above changes, $\Delta a/a_0$, could not be scaled by the electronic energy deposition at the surface.

(3) In the 100–300 MeV iodine irradiation, the lattice parameter change slightly increased with increasing incident ion energy. This tendency is opposite to the decreasing tendency of the nuclear energy deposition, but is consistent with the increasing tendency of the electronic energy deposition at the surface.

Results (1) and (2) indicate that the defect formation corresponding to the lattice parameter change was mainly due to the nuclear energy deposition. At the same time,

result (3) suggests an additional contribution of the electronic energy deposition to the defect formation, in particular, at the higher energies of 200 and 300 MeV.

Acknowledgements

The authors are deeply indebted to Dr T. Aruga of JAERI for the EDEPJR-87 code calculation and his helpful advice on the theoretical calculation, and to S. Ichikawa and K. Tsukada of the Isotope Research and Development Division, C. Kobayashi, T. Yoshida and members of the Accelerators Division of JAERI for their help in the Tandem Accelerator experiments. The authors are also indebted to T. Shiratori and S. Kashimura and Dr H. Serizawa of JAERI, as well as M. Inoue, M. Kawabe and K. Maejima of the Tokyo Nuclear Service Ltd. for their assistance in the accelerator experiment. The authors also wish to express their gratitude to Dr Hj. Matzke of the European Institute for Transuranium Elements for his helpful advice and to Dr M. Hoshi and Dr T. Muromura of JAERI for their encouragement.

Appendix A. On the revision of results for 100 MeV iodine irradiation

The previous paper [6] was made with the data for 100 MeV iodine irradiation into *unannealed* UO_2 specimens. Subsequently, repeated irradiation experiments were made at this energy with *annealed* specimens over a wide fluence range [8], and X-ray analyses were made using a molybdenum mask with a smaller slit hole (2 mm ∅) than that for the present paper (3 mm ∅). No significant difference was observed in the lattice parameter change behavior for the un-annealed [6] and annealed [8] specimens, as far as the irradiation temperature was suppressed below 200°C.

Unfortunately, however, some scattering in the lattice parameter data was observed [8], probably due to somewhat inhomogeneous distribution of the ion-beam current profile within the ion-beam spot in this case. Therefore, X-ray analyses were made again for the specimens, using a mask with a wider slit hole, 3 mm in diameter, which was more appropriate to obtain the values averaged over a wider ion-beam area, leading to reduce the scattering. Thus, the revised data plotted in Figs. 3–5 were obtained for the 100 MeV iodine irradiation.

Accordingly, the dpa scaling in Fig. 3 was made with an increased number of more reliable data in the present paper than those in the previous annual report [7]. As a consequence, the present paper offered better agreement between the data plots for the iodine and nickel irradiation.

References

[1] Hj. Matzke, these Proceedings, p. 170.
[2] Hj. Matzke, J. Nucl. Mater. 189 (1992) 141.
[3] Hj. Matzke, A. Turos, G. Linker, Nucl. Inst. Meth. B91 (1994) 294.
[4] J. Rest, G.L. Hofman, J. Nucl. Mater. 210 (1994) 187.
[5] K. Nogita, K. Une, J. Nucl. Mater. 226 (1995) 302.
[6] K. Hayashi, H. Kikuchi, K. Fukuda, J. Alloys Compounds 213&214 (1994) 351.
[7] K. Hayashi, H. Kikuchi, T. Shiratori, K. Fukuda, Radiation damage of UO_2 by 100 MeV iodine, nickel and chlorine ions, Japan Atomic Energy Research Institute Report JAERI-M 93-174 (1993) p. 63.
[8] K. Hayashi, H. Kikuchi, K. Fukuda, Radiation damage of UO_2 implanted with 100 MeV iodine ions up to fluences over an extended range, Japan Atomic Energy Research Institute Report JAERI-Review 94-008 (1994) p. 82.
[9] K. Hayashi, H. Kikuchi, K. Fukuda, Depth profile measurement of lattice parameter changes of UO_2 irradiated with 100 MeV iodine ions, Japan Atomic Energy Research Institute Report JAERI-Review 95-017 (1995) p. 79.
[10] T. Aruga, K. Nakata, S. Takamura, Nucl. Inst. Meth. B33 (1988) 748.
[11] I. Manning, G.P. Mueller, Comput. Phys. Commun. 7 (1974) 85.
[12] C.M. Davisson, I. Manning, Comput. Phys. Commun. 42 (1986) 137.
[13] M.T. Robinson, I.M. Torrens, Phys. Rev. B9 (1974) 5008.
[14] J. Soullard, J. Leteurtre, J.P. Genthon, M. Cance, Radiat. Eff. 38 (1978) 119.
[15] J. Soullard, A. Alamo, Radiat. Eff. 38 (1978) 133.
[16] M. Yoneyama, S. Sato, H. Ohashi, T. Ogawa, A. Ito, K. Fukuda, Migration behavior of palladium in UO_2 (III), Japan Atomic Energy Research Institute Report JAERI-M 92-118 (in Japanese) (1992) p. 13.
[17] Hj. Matzke, A. Turos, J. Nucl. Mater. 114 (1986) 349.
[18] W.A. Young, L. Lynds, J.S. Mohl, G.G. Libowitz, An X-ray and density study of nonstoichiometry in uranium oxides, Atomics International (AEC Research and Development Report) NAA-SR-6765 (1962).
[19] D.R. Lide, ed., CRC Handbook of Chemistry and Physics, 73rd Ed. (CRC, Boca Raton, FL, 1992) pp. 10-293 and 10-295.
[20] N. Nakae, A. Harada, T. Kirihara, S. Nasu, J. Nucl. Mater. 71 (1978) 314.
[21] Hj. Matzke, A. Turos, J. Nucl. Mater. 188 (1992) 285.